

Non-linear current–voltage characteristics of $(\text{La}_{0.5}\text{Eu}_{0.5})_{0.7}\text{Pb}_{0.3}\text{MnO}_3$ single crystals: Possible manifestation of the internal heating of charge carriers

K.A. Shaykhutdinov^{a,b}, S.I. Popkov^{a,b}, D.A. Balaev^{a,b}, S.V. Semenov^a, A.A. Bykov^a, A.A. Dubrovskiy^{a,b,*}, N.V. Sapronova^a, N.V. Volkov^{a,b}

^a Kirensky Institute of Physics, Russian Academy of Sciences, Siberian Branch, Krasnoyarsk 660036, Russia

^b Siberian Federal University, Krasnoyarsk 660041, Russia

ARTICLE INFO

Article history:

Received 3 August 2010

Received in revised form

29 September 2010

Accepted 30 September 2010

Keywords:

Manganites

Negative differential resistance

CVC

ABSTRACT

Temperature evolution of the current–voltage characteristics (CVCs) of a single-crystal lanthanum manganite $(\text{La}_{0.5}\text{Eu}_{0.5})_{0.7}\text{Pb}_{0.3}\text{MnO}_3$ is investigated in a wide (up to 1 A) range of instrumental currents. Effects of a transport current and an applied electric field on the resistance of the material are studied in view of possible implementation of the charge ordering break in dielectric regions occurring due to phase separation in manganites. A negative differential resistance portion observed in the CVCs suggests the presence of a current switching effect. Below the temperature of the metal–dielectric transition in $(\text{La}_{0.5}\text{Eu}_{0.5})_{0.7}\text{Pb}_{0.3}\text{MnO}_3$, the hysteresis is observed in the CVC. The detailed analysis of the internal sample heating on the basis of experimental data on thermal conductivity showed, however, that these CVC features can be explained within the concept of non-equilibrium heating of electron gas.

© 2010 Elsevier B.V. All rights reserved.

1. Introduction

Substituted manganese oxides, or manganites, $\text{R}_{1-x}\text{A}_x\text{MnO}_3$ where R is a trivalent rare-earth ion (La^{3+} , Nd^{3+} , Pr^{3+} , Sm^{3+} , etc.) and A is a divalent ion (Ca^{2+} , Sr^{2+} , Ba^{2+} , and Pb^{2+}) still have been a subject of intense research as the materials with rich phase diagram and physical properties sensitive to external factors such as magnetic and electric fields, transport current, and optical radiation [1–6]. These features make the manganites promising for applications in spintronic devices. Various physical properties of the manganites are associated with submicron-scale impurity phase separation [5,6] that is generally implemented as the coexistence of a conductive ferromagnetic phase and a dielectric phase with localized carriers. The colossal magnetoresistance effect typical of the manganites is caused by increasing fraction of the conductive ferromagnetic phase under the action of a magnetic field [1,5,6]. The ground state of the substituted manganites is determined by cation atomic radii in R positions and by disordering [1]. The latter may be ferromagnetic metal and antiferromagnetic with charge ordering, as in the $\text{Pr}_{0.65}(\text{Ca}_x\text{Sr}_{1-x})_{0.35}\text{MnO}_3$ [7] and $\text{La}_{0.7-x}\text{Nd}_x\text{Pb}_{0.3}\text{MnO}_3$ [8] systems. Such a change in the ground state of the manganites on doping is related to the competition of different interactions with close energy values, which allows the

system to retain the phase separation state with two coexisting phases characterized by different magnetic and electron properties. This makes it possible to vary the properties of a system by external factors.

As is known, an applied electric field or transport current strongly affects volumetric ratio of the conductive to dielectric phase [3,4,9–12]. For example, a strong dependence of resistance on the transport current was reported and called the colossal electrical resistance effect [11].

In this work, the effect of the transport current and electric field on the resistance of the manganites was studied in a single-crystal $(\text{La}_{0.5}\text{Eu}_{0.5})_{0.7}\text{Pb}_{0.3}\text{MnO}_3$ sample. The choice of this compound was based on the following. Previously, it was established [1] that in the characterized and investigated $(\text{La}_{1-x}\text{Eu}_x)_{0.7}\text{Pb}_{0.3}\text{MnO}_3$ ($x=0, 0.2, 0.4$, and 0.6) single crystals Eu ions are trivalent. Substitution of europium ions with smaller ionic radii lanthanum ions induces local distortions of Mn–O–Mn bonds in the crystal, which causes random distribution of the value and sign of the exchange interaction over the crystal volume. The competition of the exchange interactions leads to the occurrence of inhomogeneous magnetic states in the manganite samples doped by europium ions. The Curie temperature T_C decreases and the area of the inhomogeneous state existence broadens with increase in Eu concentration. For all the samples, in the area of the inhomogeneous state the colossal magnetoresistance effect is observed. For the crystals with $x=0$ – 0.5 both above and below the temperature of the magnetic phase transition, the paramagnetic phase with polaron conductivity coexists with the ferromagnetic phase with metal conductivity. The sample with $x=0.5$ at $T < T_C$ is

* Corresponding author at: Russian Academy of Sciences, Kirensky Institute of Physics, Akademgorodok, 50 Siberian Branch, 660036 Krasnoyarsk, Russian Federation. Tel.: +7 3912494838.

E-mail addresses: smp@iph.krasn.ru, andre-do@yandex.ru (A.A. Dubrovskiy).

in the inhomogeneous state where two ferromagnetic phases with different conductivities coexist. The coexisting phases are observed as spatially separated due to frustration of the antiferromagnetic and ferromagnetic interactions at the interface between the phases. The sample with $x=0.6$ does not exhibit the maximum resistance at the temperature of the metal–dielectric transition; its resistance grows with decrease in temperature. Correspondingly, the sample with $x=0.5$ is at the substitution series edge where the metal–dielectric transition is still observed but the magnetoresistance (MR) effect is maximum. We chose this sample for the measurements of the current–voltage characteristics.

2. Experimental

A single-crystal sample with $(\text{La}_{0.5}\text{Eu}_{0.5})_{0.7}\text{Pb}_{0.3}\text{MnO}_3$ composition was grown by spontaneous crystallization. Compounds PbO and PbF_2 were used as solvents and simultaneously ensured the required number of Pb ions in the crystals. The single crystals were $2 \times 2 \times 2 \text{ mm}^3$ cubic with a black glare surface and sharp edges. All the measurements were performed on the well-polished plate samples with dimensions of $1 \times 1 \times 0.5 \text{ mm}^3$. X-ray diffraction studies of the crystal showed only the perovskite-like phase with no inclusions. All the diffraction maxima belong to the structure with a P4/m space group (lattice parameters $a=b=3.88 \text{ \AA}$ and $c=3.87 \text{ \AA}$), while the initial $\text{La}_{0.7}\text{Pb}_{0.3}\text{MnO}_3$ compound has a rhombohedral structure with $R\bar{3}c$ space group (lattice parameters $a=5.523 \text{ \AA}$ and $c=13.402 \text{ \AA}$).

Temperature dependences of resistance $R(T)$, thermal conductivity $k(T)$, and magnetization $M(T)$ and $M(H)$ were measured using a PPMS–6000 facility (Quantum Design) in external magnetic fields up to 9 T. The resistance measurements in external magnetic fields up to 25 T were performed in the pulse mode using a facility for studying the physical properties of solids in strong pulse magnetic fields (Kirensky Institute of Physics). Resistance values R were determined from isotherms in the field $H=25 \text{ T}$. The current–voltage characteristics up to high instrumental transport currents (1 A) were measured by a standard four-probe method in the applied bias current regime; a Keithley-2430 current source was used as a current controller and potential drop was measured with an Agilent-34410A voltmeter. During the CVC measurements, the sample was placed in a liquid medium to avoid possible self-heating and contact heating. As refrigerants, liquid nitrogen ($T_{\text{boil}}=77.4 \text{ K}$) and ethyl alcohol (with melting temperature $T_{\text{melt}}=159 \text{ K}$ and molar specific heat under standard conditions $C_p=298 \text{ J/moleK}$) were used. The use of ethyl alcohol allowed the measurement of CVCs in a wide temperature range up to room temperature with the sample being always immersed in a liquid medium. During the measurements of the CVCs, in a dewar being pumped where temperature stabilization was implemented by helium gas circulation, typical sample self-heating was observed at which transport current fixation led either to the growth of the metal–dielectric transition temperature (below T_{max}) or to a decrease in resistance ($T \geq T_{\text{max}}$). We also observed a broad temperature hysteresis and simultaneous increase in temperature of the temperature sensor placed near the sample. The measurements were performed both at a constant current scan and in a pulse mode with a rectangular pulse duration from 200 ms to 1 s. No effect of current scan modes on the CVC shape was found. It should be noted that during the measurements (one CVC measurement being 5–60 s long) no visible boiling or even convection traces of ethyl alcohol were observed, which indicates the constant thermodynamic equilibrium temperature of a sample being measured.

In order to study the effect of an external electric field on the CVC shape, we fabricated a cell consisting of capacitor planes between which an isolated sample with terminals was placed. The interplane distance was about 1.2 mm and the maximum applied voltage was 325 V. Note that no effect of an external electric field on the CVC shape was found either.

3. Results and discussion

Fig. 1 depicts temperature dependences of resistance R of the single-crystal $(\text{La}_{0.5}\text{Eu}_{0.5})_{0.7}\text{Pb}_{0.3}\text{MnO}_3$ sample in constant external magnetic fields of 0–9 T and pulse magnetic fields up to 25 T, which correspond to complete saturation of the magnetoresistive effect. Values of the magnetoresistive effect $MR = \Delta R(H)/R(0)$ (%) are presented in the insert in Fig. 1. The temperature of the metal–dielectric transition at $H=0 \text{ T}$ for this sample is $T_{\text{max}} \approx 185 \text{ K}$. The magnetoresistive effect is observed over the entire temperature range of 2–300 K. Magnetic measurements (Fig. 2) yield $(\text{La}_{0.5}\text{Eu}_{0.5})_{0.7}\text{Pb}_{0.3}\text{MnO}_3$ Curie temperature T_C of about 215 K. According to the phase diagram presented in Ref. [1] and the magnetic and transport measurement data, one may conclude that the ferromagnetic conductive regions exist over the entire

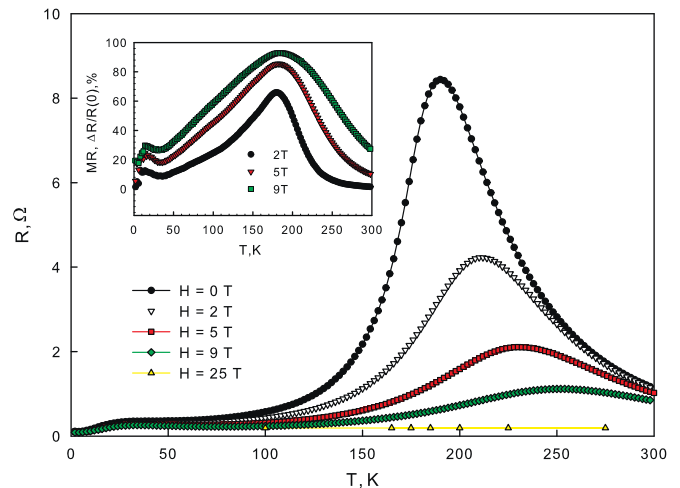


Fig. 1. Temperature dependences of resistance $R(T)$ of the single-crystal $(\text{La}_{0.5}\text{Eu}_{0.5})_{0.7}\text{Pb}_{0.3}\text{MnO}_3$ sample at constant external magnetic fields of 0–9 T and pulse magnetic fields up to 25 T.

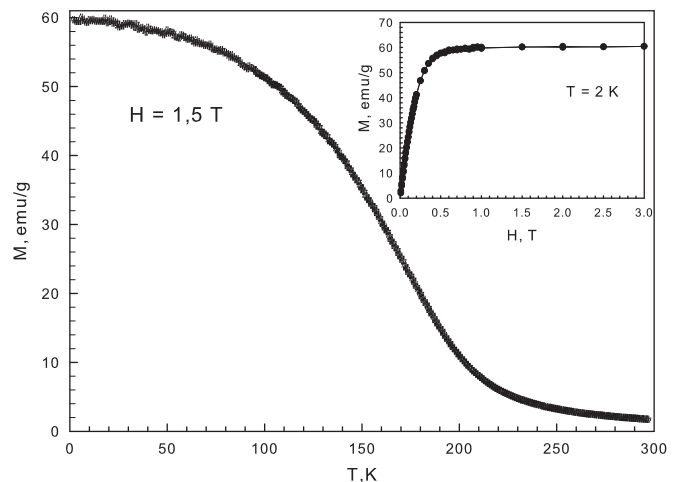


Fig. 2. Temperature dependence of magnetization $M(T)$ of $(\text{La}_{0.5}\text{Eu}_{0.5})_{0.7}\text{Pb}_{0.3}\text{MnO}_3$; insert: field dependence of magnetization $M(H)$ at $T=2 \text{ K}$.

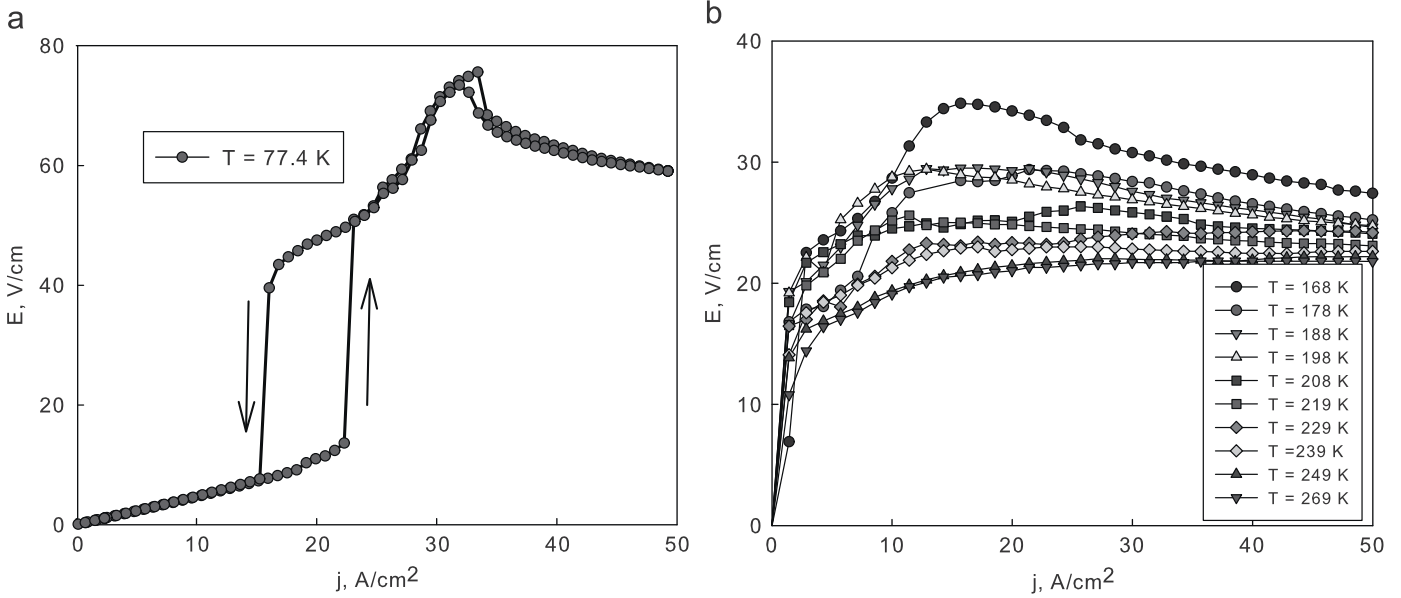


Fig. 3. Experimental current–voltage characteristics (CVCs) of $(\text{La}_{0.5}\text{Eu}_{0.5})_{0.7}\text{Pb}_{0.3}\text{MnO}_3$ measured at different temperatures: (a)—at liquid nitrogen temperature and (b)—the family of the CVCs measured in ethyl alcohol at different temperatures.

measuring temperature range, both above and below the $(\text{La}_{0.5}\text{Eu}_{0.5})_{0.7}\text{Pb}_{0.3}\text{MnO}_3$ Curie temperature, which is proved by the presence of the magnetoresistive effect. Fig. 3a and b depicts the experimental CVCs of the sample under study taken at different temperatures: nitrogen boiling temperature (Fig. 3a) and CVC temperature evolution in the temperature range 168–269 K (Fig. 3b) with ethyl alcohol as a refrigerant. At the temperature $T=77.4$ K (Fig. 3a), the CVC has a linear portion at small transport currents; then, the hysteresis feature is seen, followed by a negative differential resistance portion. The family of the CVCs measured in ethyl alcohol at different temperatures is also characterized by the presence of a negative differential resistance portion, but at these temperatures no hysteresis feature is observed; thus, in the $(\text{La}_{0.5}\text{Eu}_{0.5})_{0.7}\text{Pb}_{0.3}\text{MnO}_3$ CVC the current switching effect is observed at which the differential resistance of the sample drastically changes at certain values of the applied voltage or transport current. Similar behavior of the CVCs was reported by many authors on bulk, film, and single-crystal manganites [3,4,10–13] and other oxides [14]. In the case of the manganites, the negative differential resistance portions in the CVCs may be attributed to injection of carriers from the dielectric antiferromagnetic or ferromagnetic regions to the conductive ferromagnetic regions under the action of the external electric field, which causes an increase in conductivity of a material [3,10,11]. However, our studies on the $(\text{La}_{0.5}\text{Eu}_{0.5})_{0.7}\text{Pb}_{0.3}\text{MnO}_3$ sample with the applied electric field of the intensity $E=2.7$ kV/cm showed no effect of the electric field on the CVC shape.

In our case, the feature observed in the CVCs might be explained by internal self-heating of carriers during the measurements. Prior to the detailed consideration of the effect of the sample overheating, let us analyze the data on $(\text{La}_{0.5}\text{Eu}_{0.5})_{0.7}\text{Pb}_{0.3}\text{MnO}_3$ thermal conductivity presented in Fig. 4. As is known, the manganites have very low thermal conductivity close to the minimum theoretical value for solids [15]. It was established that the low thermal conductivity may be caused by strong phonon scattering on the defects of a crystal lattice. Using the data from Fig. 4, we can estimate thermal conductivity $\kappa_e(T)$ (in our case, $\kappa_e(T) < 0.01\kappa(T)$) in accordance with the Wiedemann–Franz law.

Denote a mean time between collisions of carriers with one another as τ_{cc} and a mean time of phonon scattering on defects of a crystal lattice as τ_{ph} . Since scattering on defects makes the major

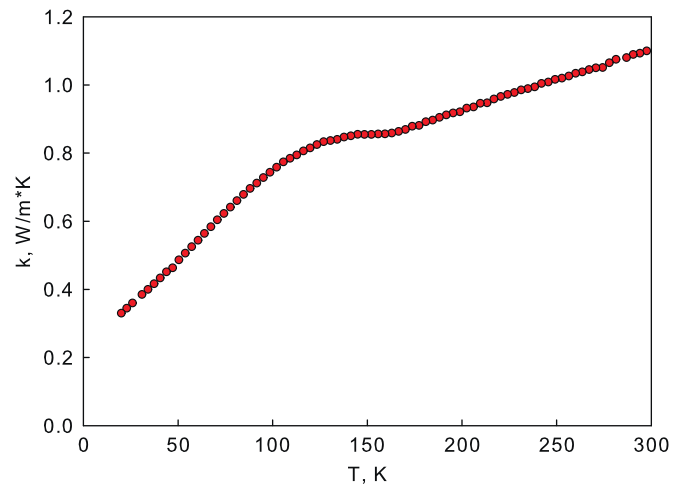


Fig. 4. Data of $(\text{La}_{0.5}\text{Eu}_{0.5})_{0.7}\text{Pb}_{0.3}\text{MnO}_3$ thermal conductivity at $H=0$ T.

contribution to thermal conductivity [15], we may conclude, based on the Wiedemann–Franz law, that the following relation between the characteristic times is valid:

$$\tau_{cc} \ll \tau_{ph} \tag{1}$$

The situation is analogous to that reported in Ref. [16], where non-equilibrium electron gas heating in semiconductors is considered causing the creation of hot electrons. Since in our case relation Eq. (1) is valid, the carriers accelerated under the action of the electric field have time to exchange energy and momentum before scattering on phonons and lattice defects play their roles. Thus, the charge carrier gas may be considered as an independent thermodynamic subsystem weakly interacting with the lattice. In this case, charge carrier temperature T_{cc} may strongly differ from lattice temperature T , which will be a thermodynamically equilibrium temperature here. Such overheating of the electron gas yields the CVC with the negative differential resistance portions. Due to fluctuations in concentration and temperature of electrons in the sample with a semiconductor-type temperature dependence of resistance, the current flow is

inhomogeneous. The sample is divided into weak and strong current regions. The strong current regions form cylindrical current streams inside the sample volume, and the final electron gas temperature is determined by heat exchange with the rest of the volume and a refrigerant [16,17]. The same approach of hot electrons was used by authors of Ref. [18] to explain non-linear transport in $\text{La}_{0.82}\text{Ca}_{0.18}\text{MnO}_3$ and $\text{Nd}_{0.7}\text{Pb}_{0.3}\text{MnO}_3$ single-crystal.

Thus, the qualitative analysis of the CVC and temperature dependence of thermal conductivity of single-crystal $(\text{La}_{0.5}\text{Eu}_{0.5})_{0.7}\text{Pb}_{0.3}\text{MnO}_3$ allow us to draw a conclusion that such a system can undergo the strong overheating of charge carriers, which leads, in the long run, to the formation of a stable strongly inhomogeneous carrier flow along the current streams whose cross section is determined by the carrier gas temperature. Let us pay attention to the $R(T)$ dependence of $(\text{La}_{0.5}\text{Eu}_{0.5})_{0.7}\text{Pb}_{0.3}\text{MnO}_3$. Consider the case when the CVCs are taken at a temperature below the maximum temperature of the metal–dielectric transition. Since the resistance grows with carrier temperature, the formation of the inhomogeneous flow is unfavorable for the system and the entire sample volume is involved in the current transfer. However, after temperature T_{cc} has exceeded $T_{max} \approx 185$ K, the resistance starts decreasing, so it becomes more favorable to reduce cross-sectional area S of the sample in order to enhance Joule heat release and to decrease the resistance by this means. Thus, the current streams start forming in the sample, i.e., the situation is analogous to that observed on the overheating of semiconductors and metals [16,17].

Now, estimate quantitatively internal overheating of the sample by simple relations analogous to those employed in Ref. [14] with no use of the exact math required in the case of bulk samples [19]. Using the Fourier thermal conductivity equation, the overheating of current carriers on simple Joule heating can be estimated as

$$\Delta T = P\ell / (kS)$$

where P is the power released in the sample at the current passage, ℓ the current channel length, k the thermal conductivity of the sample, and S the total cross-sectional area of all the current channels. Generally speaking, all the variables in this expression are functions of temperature; therefore the exact calculation requires their temperature dependences. The final temperature of a current channel is

$$T_{fin} = T_0 + \Delta T$$

where T_0 is the initial temperature, i.e., the CVC measuring temperature; thus, we can estimate the overheating of a current channel in the sample as

$$T_{fin}(E) = T_0 + E^2 \ell^3 (T) [R(T)k(T)S(T)]^{-1} \quad (2)$$

where E is the electric-field strength and $R(T)$ and $k(T)$ are the experimental temperature dependences of the resistance and thermal conductivity of the sample. As the contribution of electron thermal conductivity is small here and the transfer is totally concentrated inside the current channels, the sample volume and not the refrigerant serves as a heat-remover. In this study, we did not directly determine ℓ and S values, unlike, for example, the work shown in Ref. [2], where they were obtained by the visualization of the conductive channels. For estimation, parameter ℓ may be taken equal to the distance between potential contacts and S may be considered as a fitting parameter, not higher than the sample cross-sectional area. Fig. 5 depicts the simulation results for the overheating of a current stream by Eq. (2) for different initial temperatures. During simulation, we used the fitting parameter $S/\ell = 0.25$ cm close to the sample geometrics. This parameter determined the maximum strength in Fig. 5 corresponding to the CVC transition to the negative

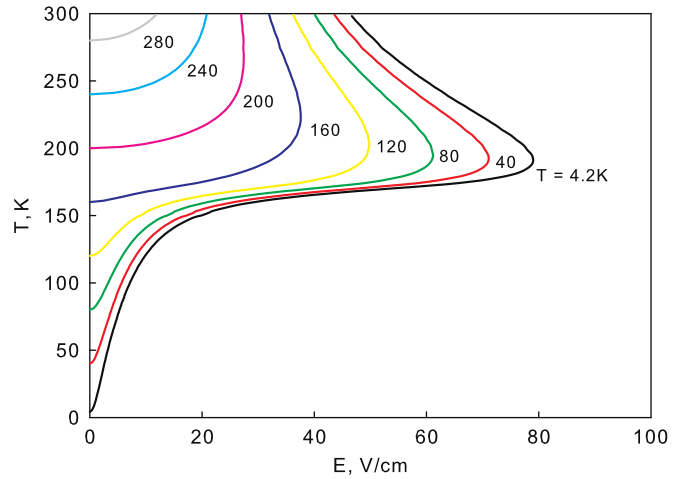


Fig. 5. Simulation results for the overheating of a current stream by expression (2) for different initial temperatures.

differential resistance portion. Simulation results allow us to conclude that at electric-field strength values of tens of V/cm, the overheating of the sample at hundreds of degrees takes place. The overheating becomes most rapid upon approaching the temperature of the metal–dielectric transition from the low-temperature region with $dT/dE > 0$. With a further increase in temperature, the overheating rate decreases, as the resistance of the samples starts dropping ($dT/dE < 0$). One can see in Fig. 5 that within the proposed consideration the CVCs measured at the temperatures below the maximum temperature of the metal–dielectric transition will have the hysteresis feature. It follows from the fact that at T_0 below the temperature of the metal–dielectric transition (Fig. 1) the $T(E)$ function becomes double-valued. This is confirmed by the CVC measurements at the liquid nitrogen boiling point (Fig. 3a). The obtained $T(E)$ dependences allow to obtain approximate $E(I)$ dependences if each E value at a given temperature is associated with an R value (Fig. 1), from which an I value is determined using Ohm's law. It should be noted here that this association provides only a qualitative form of the CVCs, as the temperature dependences of the electrical resistance were measured at the current $I = 1$ mA, i.e., on the initial linear CVC portion where the overheating processes are not decisive yet. In our case, determination of real current density requires consideration of its variation with increase in temperature; nevertheless, we performed this procedure. The obtained $E(j)$ dependences are presented in Fig. 6(a) and (b). Fig. 6(b) shows the model CVCs for the temperature range $T = 168$ – 269 K; Fig. 6(a), for $T = 77.4$ K. Comparing the experimental data (Fig. 3) with the results of the calculation (Fig. 6), one can see that they are in qualitative agreement. In addition, the model CVCs reflect correctly the CVC evolution with increase in the temperature. Also, this comparison shows that the current streams in the sample overheat up to the temperatures much higher than 300 K (Fig. 3). Note that the agreement between the experimental CVC taken at $T = 77.4$ K and the calculated CVC is substantially worse. This might be related to the fact that at these temperatures the formation of the inhomogeneous flow in the sample is unfavorable, as at first the resistance grows with temperature, and the entire sample volume participates in the current transfer. In this case, it is necessary to take into account the phase separation existing in $(\text{La}_{0.5}\text{Eu}_{0.5})_{0.7}\text{Pb}_{0.3}\text{MnO}_3$ and to use in the calculation a network of elements with different temperature-dependent resistance connected parallel and in series.

Such CVCs were also observed by us on polycrystalline $\text{La}_{0.7}\text{Ca}_{0.3}\text{MnO}_3$ manganites and on a thin film with $(\text{La}_{0.75}\text{Pr}_{0.25})_{0.7}\text{Ca}_{0.3}\text{MnO}_3$

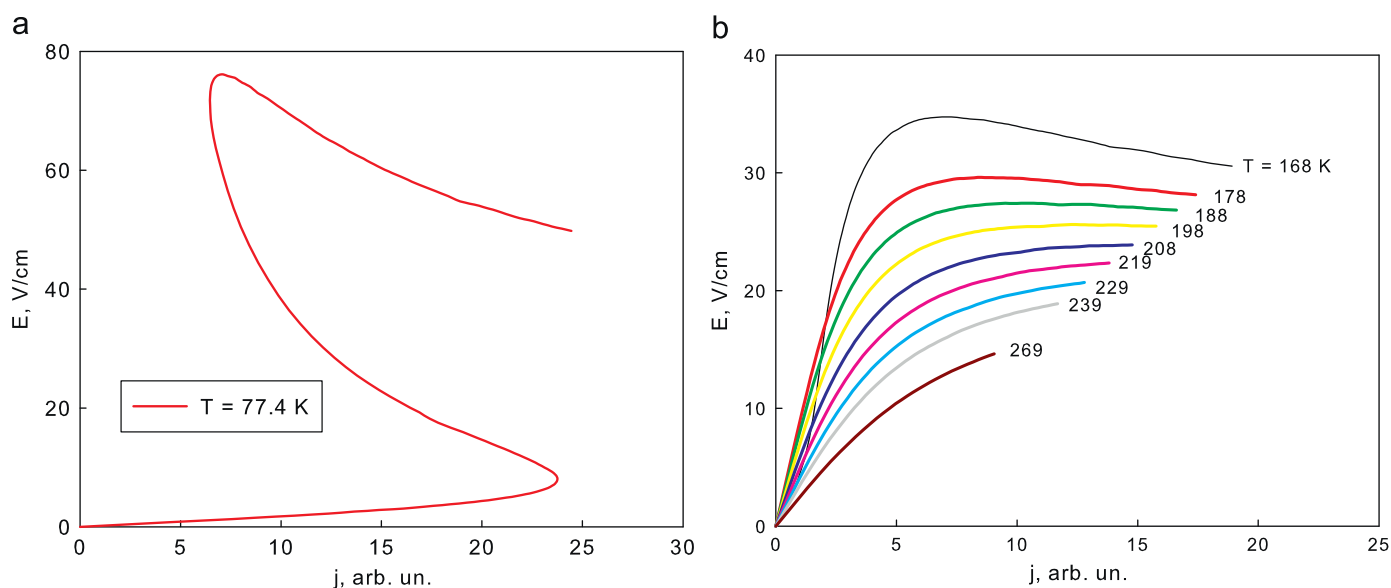


Fig. 6. Obtained $E(j)$ dependences using the simulation results according to expression (2): (a)—at liquid nitrogen temperature and (b)—model CVCs for the temperature range $T=168$ – 269 K.

composition. The features were seen in the CVCs under approximately the same conditions, which evidences the validity of the proposed model on overheating of the carriers for the manganites.

One may wonder whether a simple Joule equilibrium overheating of the sample is responsible for such non-linear effects on CVCs. So, it is instructive to estimate the characteristic time of power dissipation during measurements. We calculate the values of specific power $P=E^2/\rho$ delivered to sample at finite values of bias current density j using the data presented in Fig. 3. In the equilibrium state the heat was moved into liquid ethyl alcohol. To estimate the rate of overheating dT/dt , the simple expression $dT/dt=P/C_p$ (where C_p is molar specific heat of ethyl alcohol) was used. For example, at $j=20$ A/cm² specific power $P=1084 \pm 2$ W/cm³, using sample size $1 \times 1 \times 0.5$ mm³, power $P=0.542$ W, $dT/dt=0.0018$ K/(mole s), at $j=30$ A/cm² $P=1555 \pm 2$ W/cm³, $P=0.7775$ W, $dT/dt=0.0026$ K/(mole s), at $j=50$ A/cm² $P=2450 \pm 2$ W/cm³, $P=1.225$ W, $dT/dt=0.0041$ K/(mole s). So, during the measurements procedure the overall overheating of the sample is minor and its temperature coincides with the thermodynamic equilibrium value. This simple estimation gives additional evidence based on the above proposed model of hot electrons being responsible for non-linear effects on CVCs of $(\text{La}_{0.5}\text{Eu}_{0.5})_{0.7}\text{Pb}_{0.3}\text{MnO}_3$.

4. Conclusions

The current–voltage characteristics obtained experimentally in the single-crystal $(\text{La}_{0.5}\text{Eu}_{0.5})_{0.7}\text{Pb}_{0.3}\text{MnO}_3$ manganite were analyzed. The characteristics exhibit current switching, i.e., a hysteresis feature and a negative differential resistance portion. Results obtained show that the processes of the internal overheating of carriers at the transport current flow play an important, sometimes decisive, role in the formation of the CVCs of the materials with low thermal conductivity and specific heat such

as manganites and other oxides, including high-temperature superconductors.

Acknowledgements

The authors are grateful to A.N. Lavrov for useful discussions on the results. This study was partially supported by the Russian Foundation for Basic Research, Project no. 08-02-00259a and the Lavrent'ev Young Scientists' Competition of the Siberian Branch of the Russian Academy of Sciences, Project no. 12.

References

- [1] N. Volkov, G. Petrakovskii, K. Patrin, et al., Phys. Rev. B 73 (2006) 104401.
- [2] M. Fiebig, K. Miyano, Y. Tomioka, Y. Tokura, Science 280 (1998) 1925.
- [3] A. Asamitsu, Y. Tomioka, H. Kuwahara, Y. Tokura, Nature 388 (1997) 50.
- [4] T. Wu, J.F. Mitchell, Phys. Rev. B 74 (2006) 214423.
- [5] Y. Tokura (Ed.), Colossal Magnetoresistive Oxides, Gordon and Breach Science Publishers, 2000.
- [6] E.L. Nagaev, Usp. Fiz. Nauk 166 (1996) 833 in Russian.
- [7] H. Yoshizawa, R. Kajimoto, H. Kawano, Phys. Rev. B 55 (1997) 2729.
- [8] N. Ghosh, S. Elizabeth, H.L. Bhat, et al., Phys. Rev. B 70 (2004) 184436.
- [9] J. Gao, F.X. Hu, Appl. Phys. Lett. 86 (2005) 092504.
- [10] Z.G. Sheng, J. Gao, Y.P. Sun, Phys. Rev. B 79 (2009) 014433.
- [11] H. Jain, A.K. Raychaudhuri, N. Ghosh, H.L. Bhat, Phys. Rev. B 76 (2007) 104408.
- [12] M. Tokunaga, H. Song, Y. Tokunaga, T. Tamegai, Phys. Rev. Lett. 94 (2005) 157203.
- [13] P. Padhan, W. Prellier, Ch. Simon, R.C. Budhani, Phys. Rev. B 70 (2004) 134403.
- [14] A.N. Lavrov, I. Tsukada, Y. Ando, Phys. Rev. B 68 (2003) 094506.
- [15] A.V. Inyushkin, A.N. Taldenkov, O.Yu. Gorbenko, A.R. Kaul', Pis'ma v ZhETF 73 (2001) 689.
- [16] V.L. Bonch-Bruевич, S.G. Kalashnikov, in: Fizika poluprovodnikov, Nauka, Moscow, 1977.
- [17] V.N. Morgun, V.A. Bondar', A.M. Kadigrobov, N.N. Chebotareva, Fiz. Tverd. Tela 35 (1993) 59 in Russian.
- [18] H. Jain, A.K. Raychaudhuri, Appl. Phys. Lett. 93 (2008) 182110.
- [19] D.M. Kroll, Phys. Rev. B 9 (1974) 1669.